Please cite this article in press as: Bushi D et al. A novel histochemical method for the visualization of thrombin activity in the nervous system☆.
Neuroscience (2016), http://dx.doi.org/10.1016/j.neuroscience.2016.01.065

Neuroscience xxx (2016) xxx–xxx

A NOVEL HISTOCHEMICAL METHOD FOR THE VISUALIZATION OF THROMBIN ACTIVITY IN THE NERVOUS SYSTEM☆

D. BUSHI,[a,b*,†] O. GERA,[a,b,g†] G. KOSTENICH,[e] E. SHAVIT-STEIN,[a] R. WEISS,[a,f] J. CHAPMAN[a,b,c,d‡] AND D. TANNE[a,c‡]

[a] *Comprehensive Stroke Center, Department of Neurology and The J. Sagol Neuroscience Center, Chaim Sheba Medical Center, Tel HaShomer, Israel*

[b] *Department of Physiology and Pharmacology, Sackler Faculty of Medicine, Tel Aviv University, Tel Aviv, Israel*

[c] *Department of Neurology, Sackler Faculty of Medicine, Tel Aviv University, Tel Aviv, Israel*

[d] *Robert and Martha Harden Chair in Mental and Neurological Diseases, Sackler Faculty of Medicine, Tel Aviv University, Israel*

[e] *Advanced Technology Center, Chaim Sheba Medical Center, Tel HaShomer, Israel*

[f] *Sagol School of Neuroscience, Tel Aviv University, Tel Aviv, Israel*

[g] *Department of Physical Therapy, Sackler Faculty of Medicine, Tel Aviv University, Tel Aviv, Israel*

Abstract—Although thrombin has an important role in both central and peripheral nerve diseases, characterization of the anatomical distribution of its proteolytic activity has been limited by available methods. This study presents the development, challenges, validation and implementation of a novel histochemical method for visualization of thrombin activity in the nervous system. The method is based on the cleavage of the substrate, Boc-Asp(OBzl)-Pro-Arg-4MβNA by thrombin to liberate free 4-methoxy-2-naphthylamine (4MβNA). In the presence of 5-nitrosalicylaldehyde, free 4MβNA is captured, yielding an insoluble yellow fluorescent precipitate which marks the site of thrombin activity. The sensitivity of the method was determined *in vitro* using known concentrations of thrombin while the specificity was verified using a highly specific thrombin inhibitor. Using this method we determined the spatial distribution of thrombin activity in mouse brain following transient middle cerebral artery occlusion (tMCAo) and in mouse sciatic nerve following crush injury. Fluorescence microscopy revealed well-defined thrombin activity localized to the right ischemic hemisphere in cortical areas and in the striatum compared to negligible thrombin activity contralaterally. The histochemical localization of thrombin activity following tMCAo was in good correlation with the infarct areas per triphenyltetrazolium chloride staining and to thrombin activity measured biochemically in tissue punches (85 ± 35 and 20 ± 3 mU/ml, in the cortical and striatum areas respectively, compared to 7 ± 2 and 13 ± 2 mU/ml, in the corresponding contralateral areas; mean ± SE; $p < 0.05$). In addition, 24 h following crush injury, focal areas of highly elevated thrombin activity were detected in teased sciatic fibers. This observation was supported by the biochemical assay and western blot technique. The histochemical method developed in this study can serve as an important tool for studying the role of thrombin in physiological and pathological conditions.

Key words: ischemic stroke, thrombin, transient middle cerebral artery occlusion, crushed sciatic nerve, enzyme histochemistry.

INTRODUCTION

Thrombin has, in addition to its role in thrombogenesis, important hormone-like activities that affect various cells in the brain through the activation of its receptor, the protease-activated receptor 1 (PAR1) (Bar-Shavit et al., 1986; Coughlin, 2000; Junge et al., 2003). Activation of this receptor by low concentrations of thrombin may have neuroprotective effects while at higher concentrations thrombin has deleterious effects (Xue and Del Bigio, 2001; Noorbakhsh et al., 2003; Xi et al., 2003; Chen et al., 2010; Kameda et al., 2012). Previously, using a novel and specific biochemical method for direct quantitative detection of thrombin activity in brain slices, we have found that following both permanent (Bushi et al., 2013) and transient (Bushi et al., 2015) middle cerebral artery occlusion (MCAo) performed in mice, thrombin activity is elevated throughout the ischemic hemisphere reaching peak levels at the ischemic core. Spatial distribution analysis indicates that following transient MCAo transient middle cerebral artery occlusion (tMCAo) thrombin activity is elevated in both the infarct area and peri-infarct areas (Bushi et al., 2015). These results are in agreement with the study performed by Chen et al. showing that during acute ischemic stroke, disruption of the blood–brain

☆ This work was performed in partial fulfillment of the requirements for a Ph.D. degree by Doron Bushi and Orna Gera at the Sackler Faculty of Medicine, Tel Aviv University, Israel.

*Correspondence to: D. Bushi, Neuroscience Research Lab, Joseph Sagol Neuroscience Center, Chaim Sheba Medical Center, Tel HaShomer, Israel. Tel: +972-3-5304409; fax: +972-3-5304752. E-mail address: doron.bushi@gmail.com (D. Bushi).

† Equally contributing first authors.

‡ Equally contributing last authors.

Abbreviations: 4MβNA, 4-methoxy-2-naphthylamine; BBB, blood–brain barrier; CNS, central nervous system; MCAo, middle cerebral artery occlusion; mTBI, minimal traumatic brain injury; NAPAP, Nα-(2-Naphthylsulfonylglycyl)-4-Amidino-(D,L)-Phenylalanine Piperidide Acetate; NSA, 5-nitrosalicylaldehyde; OGD, oxygen glucose deprivation; PAR1, proteases- activated receptor 1; PBS, phosphate- buffered saline; tMCAo, transient middle cerebral artery occlusion; TTC, triphenyltetrazolium chloride.

http://dx.doi.org/10.1016/j.neuroscience.2016.01.065
0306-4522/

barrier (BBB) allows higher concentrations of blood-derived thrombin to enter the brain (Chen et al., 2012). Moreover, several *in vitro* studies have shown that thrombin is synthesized in the brain upon oxygen glucose deprivation (OGD) simulating ischemia (Thevenet et al., 2009; Stein et al., 2015). In this context, thrombin has been shown to cause synaptic dysfunction (Maggio et al., 2008; Maggio et al., 2013a,b; Becker et al., 2014; Prabhakaran et al., 2015) and later on neuronal damage (Junge et al., 2003; Suo et al., 2004; Hamill et al., 2009), through the activation of PAR1 (Chen et al., 2012). Indeed, the toxic effects of thrombin in the central nervous system (CNS) have been shown in various ischemic models, inflammatory and neurodegenerative brain diseases (Yin et al., 2010; Rami, 2012; Chapman, 2013; Davalos et al., 2014), where neuroprotection could be achieved either by PAR1 deletion as shown by the group of Traynelis (Junge et al., 2003; Hamill et al., 2009) or with thrombin inhibitors (McColl et al., 2004; Chen et al., 2012; Lyden et al., 2014).

In addition to the CNS, there are many lines of evidence suggesting that thrombin and its receptors have important roles in peripheral nerve diseases. Significant increase in thrombin-like activity was observed in sciatic nerves that were taken from rat and mice 1 and 2 days respectively after crush injury (Smirnova et al., 1996; Friedmann et al., 1999). Moreover, we have described the localization of PAR1 at the nodes of ranvier and functionally activation of these receptors results in conduction block (Shavit et al., 2008).

In contrast to immunohistochemical methods that localize the enzyme protein whether it is active or not, histochemical visualization of the activity of an enzyme is a powerful approach to study whether an enzyme is functionally involved in a pathophysiological process because it links the enzyme activity to cell and tissue structure. Although thrombin has an important role in both central and peripheral nerve diseases, characterization of the anatomical distribution of its proteolytic activity in the nervous system has been limited by available methods. With the rapid growth in the field of thrombin-based therapy it is becoming increasingly clear that the histochemical study of thrombin activity will be important in understanding the mechanisms that regulate its function during both central and peripheral nerve diseases. Recently, Chen et al. elegantly detected the location of thrombin activity in rat brains following ischemic stroke using a novel cell-penetrating peptide-imaging probe that was infused into the blood stream and then entered brain tissue through vascular disruption (Chen et al., 2012). Our study presents a new alternative method to visualize the sites of thrombin activity in all brain regions and it is not dependent on reperfusion as in the methodology of Chen et al. Moreover, this fluorescent histochemical method is relatively simple, uses commercially available products, and can be performed ex vivo with different tissue types. The method is shown to demonstrate the distribution of thrombin activity in mice brain following tMCAo and in mice sciatic nerve following crush injury.

EXPERIMENTAL PROCEDURES

The histochemical method is based on the landmark work of Dolbeare and Smith (1977). In the early stage of the development we used the commercial thrombin substrate Z-Gly-Pro-Arg-4MβNA (J-1120, Bachem, Switzerland). However, as described in the results section, we found that the specificity and sensitivity of this substrate does not fulfill the requirements for an appropriate histochemical method to localize thrombin activity. Thus, the substrate that we finally used is Boc-Asp(OBzl)-Pro-Arg-4MβNA, a thrombin substrate that was specially synthesized per our request (GL Biochem, Shanghai, China), containing the sequence Asp(OBzl)-Pro-Arg that was found to be one of the most sensitive sequences for cleavage by thrombin (Kawabata et al., 1988).

4-methoxy-β-naphthylamine (4MβNA) is a known soluble fluorophore that produces a blue fluorescence (emission = 425 nm [nm]) following excitation by wavelength of 340 [nm]. However, when 4MβNA interacts with 5-nitrosalicylaldehyde (NSA) it produces a schiff-base complex with a shift in fluorescence from yellow to orange which is water insoluble and potentially trapped in the tissue (Dolbeare and Smith, 1977; Smith, 1983; Back and Gorenstein, 1989; Cataldo and Nixon, 1990; Rudolphus et al., 1992; Kamiya et al., 1998) (Fig. 1). In our previous work we have found that thrombin activity is raised dramatically in the ischemic hemisphere 24 h following both permanent (Bushi et al., 2013) and transient (Bushi et al., 2015) MCAo. In addition, thrombin is elevated in sciatic nerves following crush injury (Smirnova et al., 1996; Friedmann et al., 1999). Thus, we assumed that thrombin that is generated in the ischemic tissue and in crushed nerve will potentially cleave the thrombin substrate Boc-Asp(OBzl)-Pro-Arg-4MβNA releasing free 4MβNA that can react with NSA to yield insoluble 4MβNA–NSA yellow fluorescent complexes marking the site of thrombin activity (Fig. 1).

Optimized substrate concentration

Since in this study we used for the first time the custom-made thrombin substrate Boc-Asp(OBzl)-Pro-Arg-4MβNA, our first step was to determine its most effective concentration. We determined this by comparing the cleavage rates of different substrate concentrations by 50 mU/ml of bovine thrombin (Sigma–Aldrich, Israel). Different concentrations of Boc-Asp(OBzl)-Pro-Arg-4MβNA substrate (0.01, 0.05, 0.1, 0.4, 0.8 mM) were added to a 96-well black microplate (Nunc, Denmark), each well in the microplate contained thrombin buffer (50 mM TRIS/HCl, pH 8.0, 0.15M NaCL, 1 mM $CaCl_2$), 0.1% BSA and 50 mU/ml of bovine thrombin. Thrombin cleaved the substrate and released free 4MβNA that was measured by a fluorescence reader (Molecular Devices, USA) with excitation and emission filters of 340 and 425 nm respectively. Cleavage rate was measured by the linear slope of the fluorescence intensity vs. time. As shown in the results section, the optimal substrate concentration was found to be 0.1 mM.

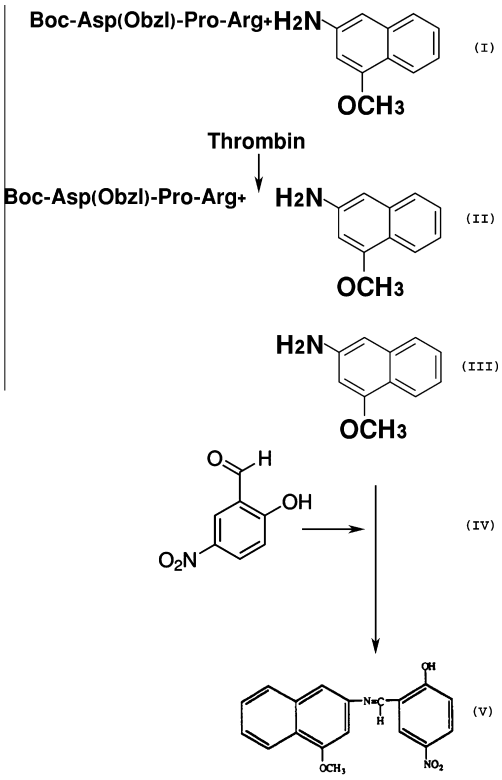

Fig. 1. Schematic diagram of the fluorescent enzyme histochemical method for the localization of thrombin activity. (I) The substrate Boc-Asp(OBzl)-Pro-Arg-4MβNA, (II) Thrombin cleaves the substrate, releases the fluorophore 4MβNA. Free 4MβNA (III) reacts with 5-nitrosalicylaldehyde (IV) to form a Schiff-base 4MβNA-NSA insoluble yellow fluorescent complexes (V) marking the sites of thrombin activity.

Assessment of the method sensitivity

In order to estimate the sensitivity of the method, we examined whether 4MβNA–NSA complexes are generated when different thrombin concentrations cleaved the Boc-Asp(OBzl)-Pro-Arg-4MβNA substrate in the presence of NSA. Eighty five microliters of thrombin buffer (50 mM TRIS/HCl, pH 7.0, 0.15M NaCL, 1 mM $CaCl_2$) were mixed with 1 microliter (0.6 mM) of NSA (Sigma–Aldrich, Israel) and 10 microliters of a range of different thrombin concentrations (2000, 250,100, 50, 25 mU/ml). As control, we used a solution containing 2000 mU/ml thrombin and NAPAP (60 μM, Nα-(2-Naphthyl sulfonylglycyl)-4-Amidino-(D,L)-Phenylalanine Piperidide Acetate, Pefabloc TH, Sigma–Aldrich, Israel) one of the most potent and selective competitive inhibitors of thrombin. Next, 5 microliters (0.1 mM) of the Boc-Asp (OBzl)-Pro-Arg-4MβNA substrate were added to the 95 microliter solution that was placed on microscopic glass slides (Superfrost Plus, Thermo Scientific, USA). The slides with the 100 microliter solution were placed in a closed tray (Humid Chamber, H-6644, Sigma–Aldrich, Israel) filled with a thin layer of water and placed at room temperature for 24 h. Later, the yellow fluorescence reactions of the generated 4MβNA–NSA complexes were photographed on an inverted fluorescence microscope (Ix81, Olympus, Japan) with a filter cube U-MWU2 (BP 300-385, BA420, DM400, Olympus, Japan). The spectra of the 4MβNA–NSA complexes were determined using a spectrometer (Glacier, BWTEK Inc, USA) at excitation $\lambda = 420$ nm (multi led light source (Prizmatix, Israel)). As shown in the results section, the 4MβNA–NSA complexes were generated in the tested thrombin range (25–2000 mU/ml).

Assessing thrombin activity levels following tMCAo and sciatic crush injury

In order to implement the histochemical method for thrombin activity staining in the nervous system we first verified using a quantitative method that the thrombin activity levels that are generated in mice brain following tMCAo and in mice sciatic nerves following crush injury are in the sensitivity range of the suggested method. Animal handling as well as all described experiments were performed in accordance and approved by the Institutional Animal Care and Use Committee of The Chaim Sheba Medical Center (Tel HaShomer, Israel), which adheres to the Israeli law on the use of laboratory animals and NIH rules.

Thrombin activity level in mouse brain following tMCAo

Studies were carried out on eight-week-old male C57BL6 mice ($n = 6$, purchased from Harlan Laboratories). Anesthesia was performed with 2.5% isoflurane mixed in oxygen and delivered through a facemask. TMCAo was performed based on our previously reported technique (Bushi et al., 2013). Briefly, a silicone-coated filament (Doccol Corp, CA, USA) was inserted through a small hole in the right external carotid artery. The filament was carefully advanced upto 11 mm from the carotid artery bifurcation or until resistance was felt. The filament was then left in place for about 90 min and then removed to achieve reperfusion. Throughout the procedure, the body temperature was kept constant at ~37 °C using a heating pad. Following surgery until recovery from anesthesia animals were kept in a closed chamber heated with a lamp. Mice were sacrificed 24 h after the procedure using pental (100 μl) by I.P. administration.

As described in our previous studies (Bushi et al., 2013), thrombin enzymatic activity was measured using a fluorometric assay based on the cleavage rate of the synthetic substrate Boc-Asp(OBzl)-Pro-Arg-AMC (I-1560, Bachem, Switzerland) and defined by the linear slope of the fluorescence intensity vs. time. Following sacrifice, the brain of each animal was immediately removed and placed in a steel brain matrix (1 mm, Coronal, Stoelting, USA). The coronal slice that is located 1 mm posterior to the bregma was removed and spatial distribution of thrombin activity in this slice was measured using the thrombin activity assay and 1-mm diameter tissue punches that were taken from 4 different locations (named A–D; Fig. 6). Each tissue sample was placed in a separate well in the 96 black microplate and thrombin activity was measured using the thrombin activity assay. Measurements were carried out using a microplate reader (Infinite 2000, Tecan, Switzerland) with excitation and emission filters of 360 ± 35 and

460 ± 35 nm, respectively. For calibration, known concentrations of bovine thrombin (Sigma–Aldrich, Israel) were used in the same assay. Following tissue samples, the punctured slices were stained using triphenyltetrazolium chloride (TTC) for infarct assessment.

Thrombin activity level in mice sciatic nerves following crush injury

Previous studies have reported that thrombin-like activity that was measured using an absorption detection method, was elevated in rat and mice sciatic nerves 1 and 2 days respectively after crush injury (Smirnova et al., 1996; Friedmann et al., 1999). In this study we used a mouse model, so we verified using a highly sensitive fluorometric method, that 24 h following sciatic crush injury thrombin activity levels in mice sciatic nerves are elevated above the sensitivity limit of the histochemical method.

Mice (n = 8) were anesthetized with a mixture of 100 mg/kg ketamine and 10 mg/kg xylazine that was injected I.P. The left thigh was cleaned by 70% ethanol, and then a small incision was made in the thigh through the connective tissue between the gluteus and the biceps femoris muscles. The sciatic nerve was exposed and tightly compressed with flattened forceps for 30 s. Immediately thereafter, the skin was sutured and the animals were placed in a closed heated chamber until recovery from anesthesia. All the surgical procedures were performed under a binocular operating microscope, while throughout the procedure, the mouse's body temperature was kept constant at ~37 °C using a heating pad. Mice were sacrificed 24 h after the procedure using pental (100 μl) by I.P. administration.

Twenty four hours following the crush procedure, both injured and contralateral uninjured sciatic nerves were isolated from the treated mice and washed with ice-cold phosphate-buffered saline (PBS). The epineurium was gently rolled-up and the fibers were placed in 96 black microplate wells. Thrombin activity was measured, as mentioned above, using thrombin activity assay based on the Boc-Asp(OBzl)-Pro-Arg-AMC substrate. Sciatic nerves that were taken from healthy control mice served as a second control. For calibration, known concentrations of bovine thrombin (Sigma–Aldrich, Israel) were used in the same assay.

Differences in thrombin activity levels between injured and contralateral uninjured nerves were confirmed using western blot technique. The epineurium of isolated sciatic nerves was gently rolled-up and the fibers were homogenized using a pestle motor mixer (Argos technologies, USA). Proteins from the sciatic homogenates (20 μg total proteins) were separated by polyacrylamide gel electrophoresis and transferred onto nitrocellulose membranes for western blot analysis. Membranes were incubated with primary goat anti thrombin antibody (1:300, sc-23335, Santa Cruz, USA) overnight with gentle agitation at 4 °C. Each injured sciatic nerve had its uninjured contralateral one serving as control. Membranes were incubated at room temperature with horseradish peroxidase-conjugated donkey anti-goat antibody (Jackson Immunoresearch Laboratories, USA) and bound antibody detected using enhanced chemiluminescence (ECL) assay kit (Thermo Scientific, USA).

Histochemical visualization of thrombin activity in mice brain following tMCAo

TMCAo was performed in eight-week-old male C57BL6 mice as described above. Mice were sacrificed 24 h after the procedure using pental (100 μl) by I.P. administration. Immediately after sacrifice the mice brains were removed and inserted into 30% sucrose solution for 24 h at 4 °C. Thereafter, the brains were cut into 20-μm coronal slices using a cryostat (Leica CM1850, Leica, Germany), and the cut sections were picked up on microscopic glass slides (Superfrost Plus, Thermo Scientific, USA). The glass slides with the fresh frozen sections were placed in a closed tray (Humid Chamber, H-6644, Sigma–Aldrich, Israel) filled with a thin water layer. For thrombin activity staining, slices that were taken from the ischemic core (~1 mm posterior to the bregma) were used. The slices were incubated in a solution containing 93 microliters of thrombin buffer (50 mM TRIS/HCl, pH 7.0, 0.15M NaCL, 1 mM $CaCl_2$), 1 microliter (0.6 mM) of NSA, 1 microliter of an aminopeptidase inhibitor bestatin (0.1 mg/ml, Cayman Chemical Company, USA) and 5 microliters (0.1 mM) of the thrombin substrate Boc-Asp(OBzl)-Pro-Arg-4MβNA. The tray with the stained slices was placed at room temperature for 24 h. In order to ensure that the localization of the histochemical reaction product specifically results from thrombin activity cleavage of the substrate the following controls were used: (1) sections were incubated in the histochemical solution containing 60 μM of the thrombin inhibitor NAPAP; (2) sections were incubated in the histochemical solution from which the NSA was omitted. The reaction was terminated by rinsing the sections in cold 50 mM TRIS/HCl, pH 7.0. Next, the sections were fixed using 4% paraformaldehyde in 0.1 M PBS, pH 7.4. Twenty minutes later, the sections were washed with PBS and 0.1% Triton X-100 (PBST) and incubated for 10 min with Hoechst (1:1000, hoe-33342, Sigma–Aldrich, Israel) for nuclear staining. After additional washing with PBST the sections were air dried and closed with mounting media and cover glass. Thrombin activity localization and hoechst staining were visualized using an inverted fluorescence microscope (Ix81, Olympus, Japan) with a filter cube U-MWU2 (BP 300-385, BA420, DM400, Olympus, Japan).

Histochemical visualization of thrombin activity in mice sciatic nerve following crush injury

Crush injury was performed in eight-week-old male C57BL6 mice as described above. Mice were sacrificed 24 h after the procedure using pental by I.P. administration. Sciatic nerves were isolated from mice and washed with ice-cold PBS. The epineurium was gently rolled-up and the fibers were teased into single fibers on microscopic glass slides (Superfrost Plus, Thermo Scientific, USA). The glass slides with the sciatic fibers were placed in a closed tray (Humid Chamber, H-6644, Sigma–Aldrich, Israel) filled with thin water layer and stained for thrombin activity as

described above using the histochemical solution. As controls, some fibers from the crushed sciatic nerves were stained with the histochemical solution and NAPAP (60 μM). In addition, fibers from the contralateral uninjured nerve were also stained for thrombin activity and served as controls.

Statistics analysis

Statistical analyses were conducted using SPSS v. 22 for Windows (IBM, NY, USA). Student t test was used to analyze differences in thrombin activity levels. All numerical data are expressed as mean ± SEM, unless otherwise indicated. *P* values of < 0.05 were considered significant.

RESULTS

Limitation of the thrombin substrate Z-Gly-Pro-Arg-4MβNA for histochemical method

The specificity of the commercially available substrate Z-Gly-Pro-Arg-4MβNA for thrombin was studied using the fluorometric assay for measuring thrombin activity in the brain and brain slices taken from the infarct core 24 h following MCAo. Briefly, mouse brain was immediately removed following sacrifice and cut into 1-mm coronal slices. Slices from the infarct core (slice # 5, #6 (1 mm posterior to the bregma) and #7) with potentially the highest amount of thrombin following MCAo were used (Bushi et al., 2013, 2015). The slices were placed into a 96-well black microplate (Nunc, Denmark) containing the substrate buffer as previously described (Bushi et al., 2013, 2015) and the Z-Gly-Pro-Arg-4MβNA substrate (0.8 mM). The thrombin in the ischemic tissues cleaved the Z-Gly-Pro-Arg-4MβNA substrate and released free 4MβNA that was measured by the fluorescence reader (Molecular Devices, USA) with excitation and emission filters of 340 and 425 nm respectively. As shown in Fig. 2, during the first 45 min a significant increase in fluorescence signal was observed. After 45 min the thrombin inhibitor - NAPAP (1 μM) was added to each well, and the fluorescence signals were not completely inhibited, demonstrating that the measured signals do not represent only thrombin activity. This experiment demonstrates the lower specificity of the substrate Z-Gly-Pro-Arg-4MβNA for thrombin. Moreover, no yellow 4MβNA–NSA complexes were generated when the Z-Gly-Pro-Arg-4MβNA substrate was incubated with NSA and high concentrations of commercial thrombin (data not shown). Based on these results, we decided to change the target substrate to a custom-made substrate containing the sequence Asp(OBzl)-Pro-Arg which has higher sensitivity (Kawabata et al., 1988) and better specificity (Bushi et al., 2013) to thrombin cleavage.

Optimized substrate concentration

The cleavage rates of the thrombin substrate Boc-Asp (OBzl)-Pro-Arg-4MβNA by 50 mU/ml of thrombin are presented as a function of different substrate concentrations (Fig. 3). The maximum cleavage rate was achieved with a substrate concentration of 0.1 mM. Interestingly, higher concentrations of the substrate inhibit the reaction. For comparison, a lower cleavage rate was measured when 50 mU/ml of thrombin cleaved the thrombin substrate Z-Gly-Pro-Arg-4MβNA (using its optimal concentration-0.8 mM), indicating the higher sensitivity of Boc-Asp(OBzl)-Pro-Arg-4MβNA for thrombin (Fig. 3).

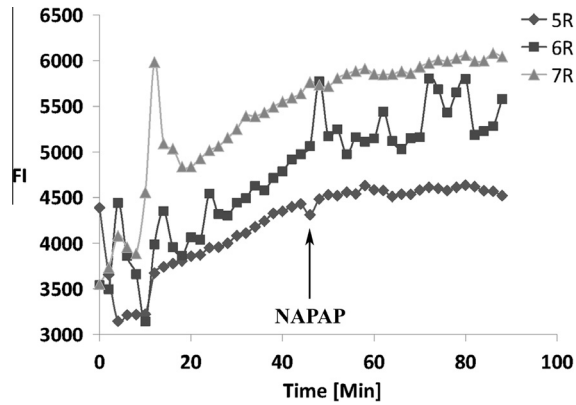

Fig. 2. Unspecific fluorescence signals with the Z-Gly-Pro-Arg-4MβNA substrate. Enzyme activity that was measured in brain slices taken from infarct core of mouse brain 24 h following MCAo. The raised signals are accumulation of free 4MβNA that were librated from the Z-Gly-Pro-Arg-4MβNA substrate. NAPAP, a specific thrombin inhibitor, was added to each well after 45 min of detection. The initial values of fluorescence intensity at time zero, related to auto fluorescence of the tested tissue. Slice thickness = 1 mm; FI = Fluorescence Intensity.

Assessment of the method sensitivity

The yellow fluorescence reaction products of the 4MβNA–NSA complexes are presented in Fig. 4. Different concentrations of thrombin (25–2000 mU/ml) cleaved the Boc-Asp(OBzl)-Pro-Arg-4MβNA substrate and liberated the 4MβNA fluorophore. Then, the 4MβNA coupled with free NSA to generate together 4MβNA–NSA insoluble complexes. As previously described, we found that the 4MβNA–NSA complexes appeared as small, discrete, yellow-orange fluorescent, needle- shaped crystals (Dolbeare and Smith, 1977; Back and Gorenstein, 1989; Cataldo and Nixon, 1990; Rudolphus et al., 1992; Kamiya et al., 1998) (Fig. 4b). The densities of the generated 4MβNA–NSA complexes are positively correlated with the thrombin concentration (Fig. 4a, d–g). Based on these findings we defined 25 mU/ml as the detection limit of the method. NAPAP, a potent and selective competitive inhibitor of thrombin, completely inhibited the reaction (Fig. 4c).

The measured fluorescence spectra of the 4MβNA–NSA complex are shown in Fig. 5. The resulting fluorescence spectrum (peaks at 530 and 595 nm) is in good agreement with the known data that the 4MβNA–NSA complex produces a shift in fluorescence of the 4MβNA to 530 and 595 nm (Dolbeare and Smith, 1977). The 530 nm peak is a blue-green nonspecific fluorescence that probably resulted from the non enzymatic reaction of NSA with amino groups to form Schiff-base adducts (Dolbeare and Smith, 1977).

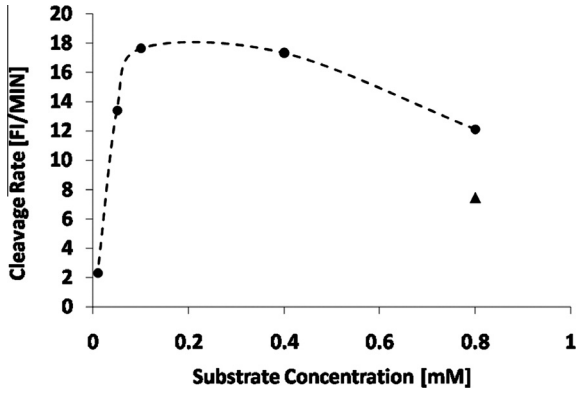

Fig. 3. The relation between the cleavage rates of the thrombin substrate and substrate concentrations. Cleavage rates of thrombin substrates (Boc-Asp(OBzl)-Pro-Arg-4MβNA, circles; Z-Gly-Pro-Arg-4MβNA, triangle) by 50 mU/ml of bovine thrombin as a function of different substrate concentrations. FI = Fluorescence Intensity.

Thrombin activity levels in mice brain following tMCAo

Twenty four hours following 90-min tMCAo, the distribution of thrombin activity levels was measured in 1-mm-thick fresh coronal slices that are located 1 mm posterior to the bregma. Based on our previous studies, in this brain area thrombin reached its maximal levels following MCAo (Bushi et al., 2013, 2015). Tissue punches were sampled from several locations in the slice including the cortex and the striatum. High thrombin values were found in locations A–D of the right ischemic hemisphere and they were significantly higher compared to the corresponding areas in the contralateral slices (61 ± 25, 20 ± 3, 73 ± 35, 85 ± 35 vs. 17 ± 3, 13 ± 2, 8 ± 3, 7 ± 2 mU/ml; mean ± SEM; $n = 6$; $p = 0.025$, 0.026, 0.026 and 0.025 respectively by paired Student t test; Fig. 6). As expected, the highest thrombin activity values were found in ischemic cortical areas (A, C and D) based on TTC staining and they were above the sensitivity limit of the histochemical method developed in this study. In contrast, lower thrombin activity levels were measured in the right striatum (location B) that included peri-infarct areas per TTC staining. These lower values are around the sensitivity limit of the histochemical method. In the contralateral hemisphere even lower levels of thrombin activity were measured in all regions and they were below the detection limit of the histochemical method.

Histochemical visualization of thrombin activity in mice brain following tMCAo

Fig. 7 presents the topographic distribution of thrombin activity following tMCAo. This a representative slide out of 15 experiments performed in a similar fashion. High density of small, discrete, yellow-orange fluorescent, needle-shaped crystals was observed in the right ischemic hemisphere in all cortical and preoptic areas (Fig. 7e, g, i) and in the striatum (Fig. 7c) compared to negligible thrombin activity contralaterally (Fig. 7b, d, f). The histochemical localization of thrombin activity corresponds to the infarct areas per TTC staining and to areas with high thrombin activity levels as determined using the thrombin activity assay and tissue punches technique (Fig. 6). In addition, the relatively lower thrombin activity levels that were measured using the punch technique in location B (20 ± 3 mU/ml, Fig. 6), are probably due to measurement of thrombin activity in borderzone areas that include both high and low thrombin levels (Fig. 7a, dashed circle). No staining was observed in the sections that were incubated with the thrombin inhibitor NAPAP (Fig. 7h) and in the sections that were incubated in the histochemical solution from which the NSA was omitted (data not shown).

Thrombin activity levels in mice sciatic nerves following crush injury

A significant increase in thrombin activity levels was observed in mice sciatic nerves 24 h following crush

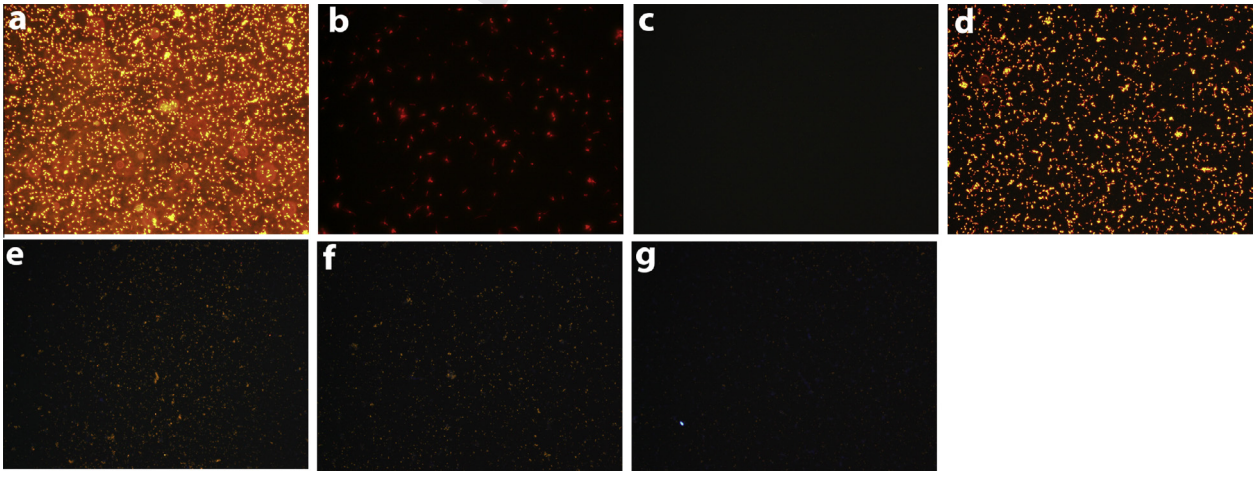

Fig. 4. Fluorescence reactions of the 4MβNA–NSA complexes as function of different thrombin concentrations. Different concentrations of bovine thrombin (25–2000 mU/ml) cleaved the Boc-Asp(OBzl)-Pro-Arg-4MβNA substrate and liberated 4MβNA that coupled with free NSA to generate r 4MβNA–NSA insoluble yellow fluorescence complexes. The densities of the generated 4MβNA–NSA complexes are positively correlated with the thrombin concentration: (a) 2000, (b) 2000 (magnification ×400), (c) 2000 + NAPAP (60 μM), (d) 250, (e) 100, (f) 50, (g) 25. All magnifications (except b) are ×100. (For interpretation of the references to colour in this figure legend, the reader is referred to the web version of this article.)

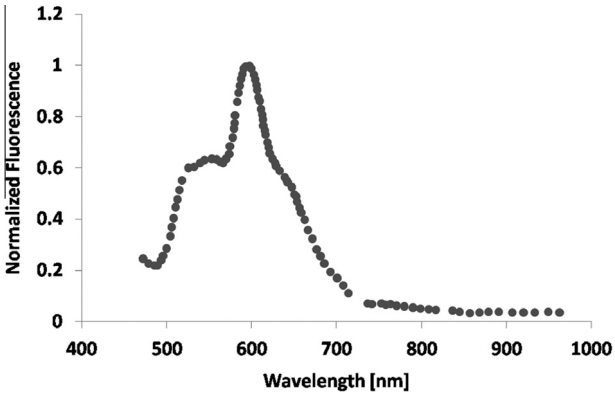

Fig. 5. Fluorescence spectra of the 4MβNA–NSA complexes. Fluorescence spectra of 4MβNA–NSA complexes that were generated during hydrolysis of Boc-Asp(OBzl)-Pro-Arg-4MβNA by 2000 mU/ml of bovine thrombin in the presence of NSA.

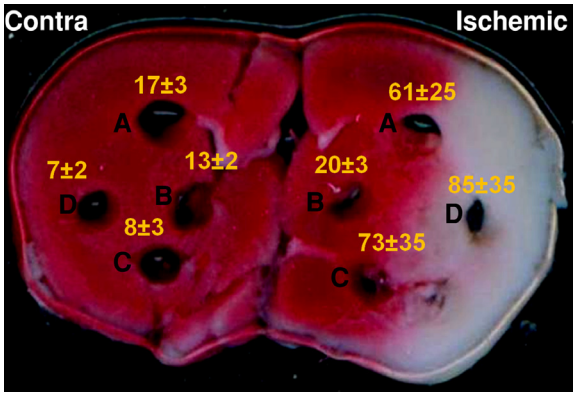

Fig. 6. Spatial distribution of thrombin activity levels and infarct area in mice brain following tMCA. Mean thrombin activity level (mU/ml of tissue ± SEM) measured at different locations in the ischemic and contralateral hemispheres following tMCAo. Typical TTC staining of the relevant slice used in these analyses is presented (representative of six slices developed by this method). Infarct regions are colored by white and intact brain regions by red. (For interpretation of the references to colour in this figure legend, the reader is referred to the web version of this article.)

injury. Thrombin activity in the injured nerve was elevated to levels of 245 ± 41 mU/ml and it was significantly higher compared to thrombin activity levels that were measured in both the uninjured contralateral sciatic nerves (27 ± 7 mU/ml, $n = 8$, $p < 0.0001$, by paired Student t test) and in control sciatic nerves that were taken from healthy control mice (28 ± 7 mU/ml, $n = 8$, $p < 0.0001$, by unpaired Student t test) (Fig. 8a). Western blotting of injured sciatic nerve samples confirmed the significantly elevated level of thrombin activity ($n = 4$, $p < 0.05$, by paired Student t test) (Fig. 8b).

Histochemical visualization of thrombin activity in mice sciatic nerves following crush injury

Fig. 9a–e depicts different examples of visualization of thrombin activity staining by histochemical staining of sciatic nerves of mice 24 h following crush injury. Only a few reaction products were seen 1 h after the reaction started (Fig. 9a) while optimal staining was observed 24 h later (Fig. 9b–e). In some cases large amounts of thrombin that were generated in the fibers diffused out to the surrounding areas (Fig. 9b, d). As expected, the reaction products appear as small, discrete, yellow-orange fluorescent, needle-shaped crystals (Fig. 9e). No staining was seen in sciatic nerves that underwent crush injury and were stained with the thrombin inhibitor NAPAP (Fig. 9f, g) and in control uninjured nerves (Fig. 9h).

DISCUSSION

The study of Dolbeare and Smith (1977) provided the impetus for studies visualizing enzymes by histochemical techniques that is based on the 4MβNA–NSA complexes. This report presents a new fluorescent enzyme histochemical method for fluorescent visualization of thrombin activity. The method was used to demonstrate the localization of thrombin activity in mice brain following tMCAo and in mice sciatic nerve following crush injury.

The specificity of this histochemical method for thrombin activity was demonstrated using NAPAP, one of the most potent and selective competitive inhibitors of thrombin (Bushi et al., 2013; Itzekson et al., 2014; Itsekson-Hayosh et al., 2015; Stein et al., 2015). NAPAP blocked the thrombin activity either when commercial thrombin was used to determine the method's sensitivity (Fig. 4c), thrombin that was generated in ischemic brain following tMCAo (Fig. 7h) or thrombin that was generated in sciatic nerve following crush injury (Fig. 9f, g). Although there are some data that trypsin-type serine proteases can also cleave the substrate Boc-Asp(OBzl)-Pro-Arg-4MβNA (Kawabata et al., 1988; Fukusen and Aoki, 1996), the sensitivity of this substrate for thrombin is much higher compared to trypsin with higher Kcat/Km ratio for thrombin (Kawabata et al., 1988). Moreover, the fact that NAPAP that its inhibition constant for thrombin is 2-fold lower than for trypsin (Sturzebecher et al., 1984), completely inhibited the substrate's cleavage, indicates that reaction products results from thrombin activity and not from trypsin. In addition, the similarity between the sequence of the Boc-Asp(OBzl)-Pro-Arg-4MβNA substrate and the amino acid order in the cleavage site of thrombin in PAR1 (. . .TL**DPR**/SFLLRNPN. . .) also provides support to the sensitivity of this substrate for thrombin. In contrast, trypsin preferentially cleaved PAR2 that has a different amino acid sequence in its cleavage site (. . .SS**KGR**/SLIGKVDGTS. . .) (Kawabata and Kuroda, 2000).

Even though the rate of coupling reaction of 4MβNA and NSA is pH dependent, we found that there is apparently sufficient formation of a stable adduct of 4MβNA and NSA at pH 7.0 to permit visualization of the thrombin activity reaction product. Although the 4MβNA–NSA complexes methodology is usually used for visualization of enzymes with optimal activity in acidic pH (Kamiya et al., 1998), in some studies (Back and Gorenstein, 1989; Rudolphus et al., 1992) this methodology was used in more neutral pH environments similar to

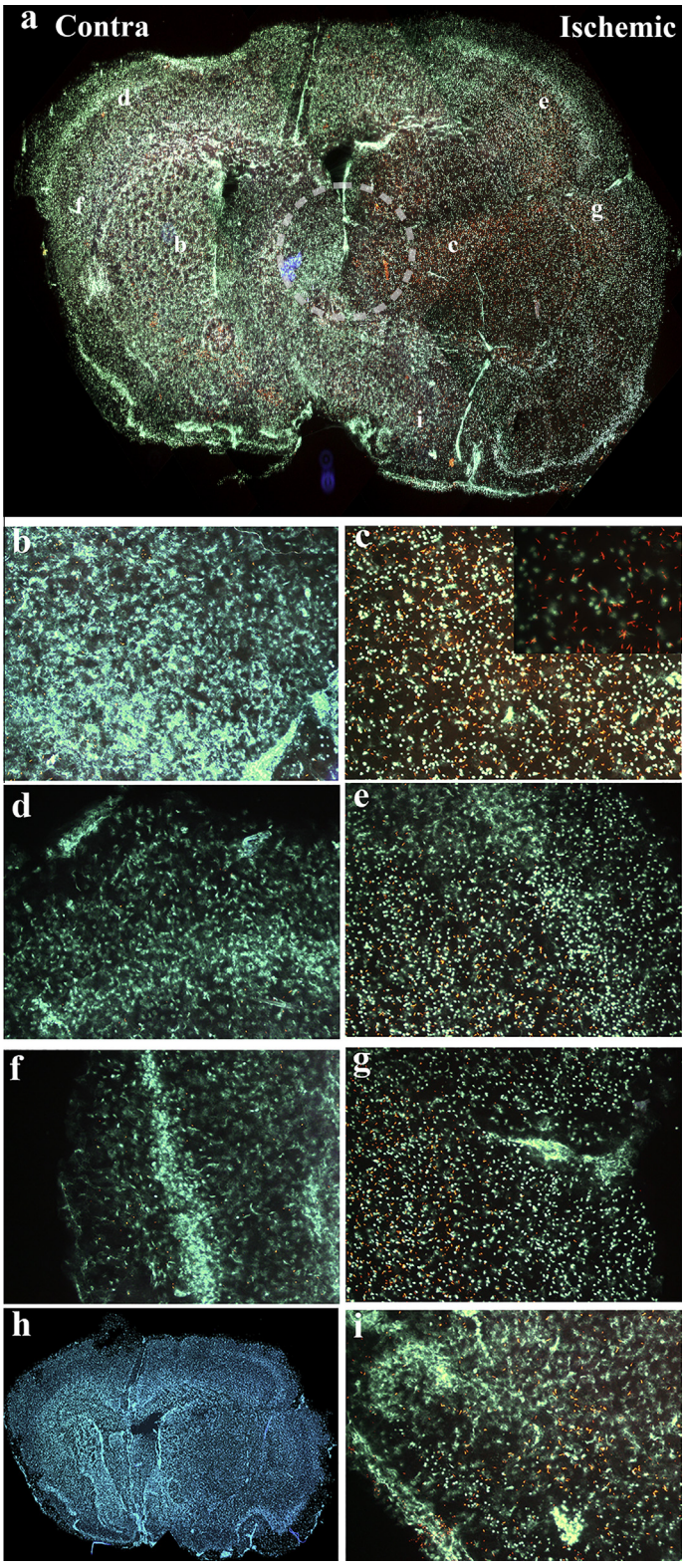

Fig. 7. Histochemical visualization of thrombin activity following tMCAo. (a) Fluorescence photomicrographs of coronal section of mouse brain following tMCAo that was incubated with Boc-Asp(OBzl)-Pro-Arg-4MβNA. Mosaic was formed by merging 20 pictures, each picture magnification ×40. Higher power photomicrograph of the typical appearance and distribution of the thrombin activity reaction product at selected areas in the ischemic hemispheres (c, e, g, i, magnification ×100). The small, discrete, yellow-orange fluorescent, needle-shaped crystals can clearly be seen in the inset picture in Fig. 7c (taken from the right ischemic striatum, magnification ×400). Negligible staining was observed in the contralateral side (b, d, f, magnification ×100). Cell nucleus was stained by hoechst and appeared as blue spots. (h) Absence of thrombin activity reaction product in tissue incubated in histochemical staining solution containing NAPAP (Mosaic was formed by merging 20 pictures, each picture magnification ×40). (For interpretation of the references to colour in this figure legend, the reader is referred to the web version of this article.)

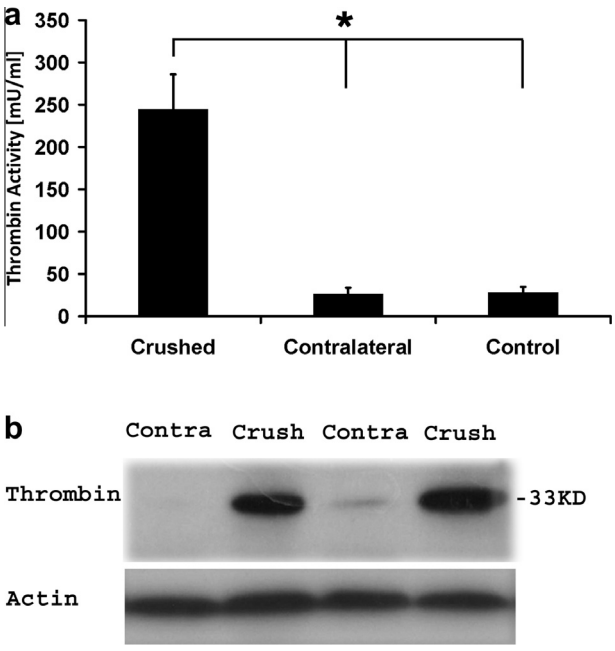

Fig. 8. Thrombin activity increased in mice sciatic nerves following crush injury. (a) Thrombin activity levels that were measured in mice sciatic nerves using thrombin activity assay ($^{*}p < 0.0001$). (b) Western blots showed a significant increase of thrombin level in crushed sciatic nerves compared with uninjured contralateral sciatic nerves.

that presented here. In the same context, the relative high detection limit of the suggested method (~25 mU/ml, Fig. 4), is probably due to the conflict between the optimal conditions of thrombin activity (~pH 8.0) to the optimal conditions for 4MβNA–NSA coupling (acid pH). We did consider modifying the method to carry out the enzymatic reaction in two stages, the thrombin substrate reaction at pH 8.0 followed by a second reaction in which NSA was added to the reaction mixture acidified to pH ~6.0 by the addition of concentrated HCl. The results of these assays (not shown) revealed that in order to obtain a specific signal, long incubation times were necessary for the thrombin reaction which would greatly reduce the spatial resolution of the method and this approach was therefore abandoned.

Similar to what was previously reported (Dolbeare and Smith, 1977), we have found that NSA has some inhibitory effect on the activity of thrombin (data not shown). In order to minimize this inhibitory effect, we used NSA concentration of 0.6 [mM] which is slightly above the minimal NSA concentration that is required by the NSA to trap all liberated 4MβNA (Back and Gorenstein, 1989).

Due to its relative lower specificity (Fig. 2) and sensitivity (Fig. 3) to thrombin, we found that the substrate Z-Gly-Pro-Arg-4MβNA is not suitable for this histochemical method. Instead, we successfully used the Boc-Asp(OBzl)-Pro-Arg-4MβNA with amino acids sequence that was found to be most sensitive for highly purified human α thrombin compared to other blood-clotting proteases (Kawabata et al., 1988). Previously, we successfully used as thrombin substrate the same Boc-Asp(OBzl)-Pro-Arg sequence coupled to the fluorophore 7-amino-4-methylcoumarin. We used this substrate in a quantitative and specific method that we developed for measurement of thrombin activity levels in brain slices (Bushi et al., 2013). We have shown that NAPAP completely inhibited the fluorescence signals that were generated when thrombin activity was measured in ischemic slices using Boc-Asp(OBzl)-Pro-Arg-AMC substrate (Bushi et al., 2013). Moreover, the Asp(OBzl)-Pro-Arg sequence is highly analogous to the known sequence of PAR1 cleaved by thrombin and may better represent the PAR1 cleaving potential of thrombin activity.

Optimal staining was observed with samples that were incubated for 24 h in room temperature. These conditions are in agreement with the work of Beck and Gorenstein that developed the histochemical method, based on 4MβNA–NSA complexes, for visualization of enkephalinase activity in rat brain (Back and Gorenstein, 1989). In contrast, different incubation conditions were used in other studies in the same field that used cells or lung tissues samples (Dolbeare and Smith, 1977; Rudolphus et al., 1992; Kamiya et al., 1998).

In the present study, we confirm our previous finding (Bushi et al., 2015) that upon a tMCAo, thrombin activity rises significantly in the ischemic hemisphere. Furthermore, spatial distribution analysis using tissue punches indicated that the highest thrombin activity levels were found in infarct areas based on TTC staining (Fig. 6). This finding also confirms a positive correlation between thrombin activity level and infarct size (Bushi et al., 2013). It seems meaningful that we have found the distribution of thrombin activity in the tested slices was similar in both the punch method and the new higher resolution histochemical method. In both methods high thrombin activity levels were observed in the right ischemic hemisphere in all cortical areas and in the striatum compared to negligible thrombin activity levels contralaterally.

In addition to the CNS, we have demonstrated the capability of this new histochemical staining to localize excess thrombin activity in the sciatic nerve following crush injury that simulates peripheral nerve disease. First, we verified using the quantitative thrombin activity assay that 24 h following crush injury, thrombin activity levels in mice sciatic nerve are elevated above the detection limit of the histochemical method (Fig. 8a). This increase in thrombin was also confirmed by western blot technique (Fig. 8b). Following staining for thrombin activity localization we have found distinct yellow–orange fluorescent products covering the nerve surfaces, while in some cases some thrombin spilled out into the surrounding areas (Fig. 9). The latter observation is in agreement with our previous finding that thrombin diffuses out from its source tissue and is detected in the surrounding buffer solution (unpublished data).

The main advantage of the histochemical method presented in this study is the ability to detect the location of thrombin activity at the cellular level. The broad emission spectrum of the 4MβNA and NSA complex (Fig. 5), makes it possible to visualize both thrombin activity and the nuclear staining by exciting both fluorophores simultaneously in the same tissue section (e.g. Fig. 7c). Localization of thrombin activity at the

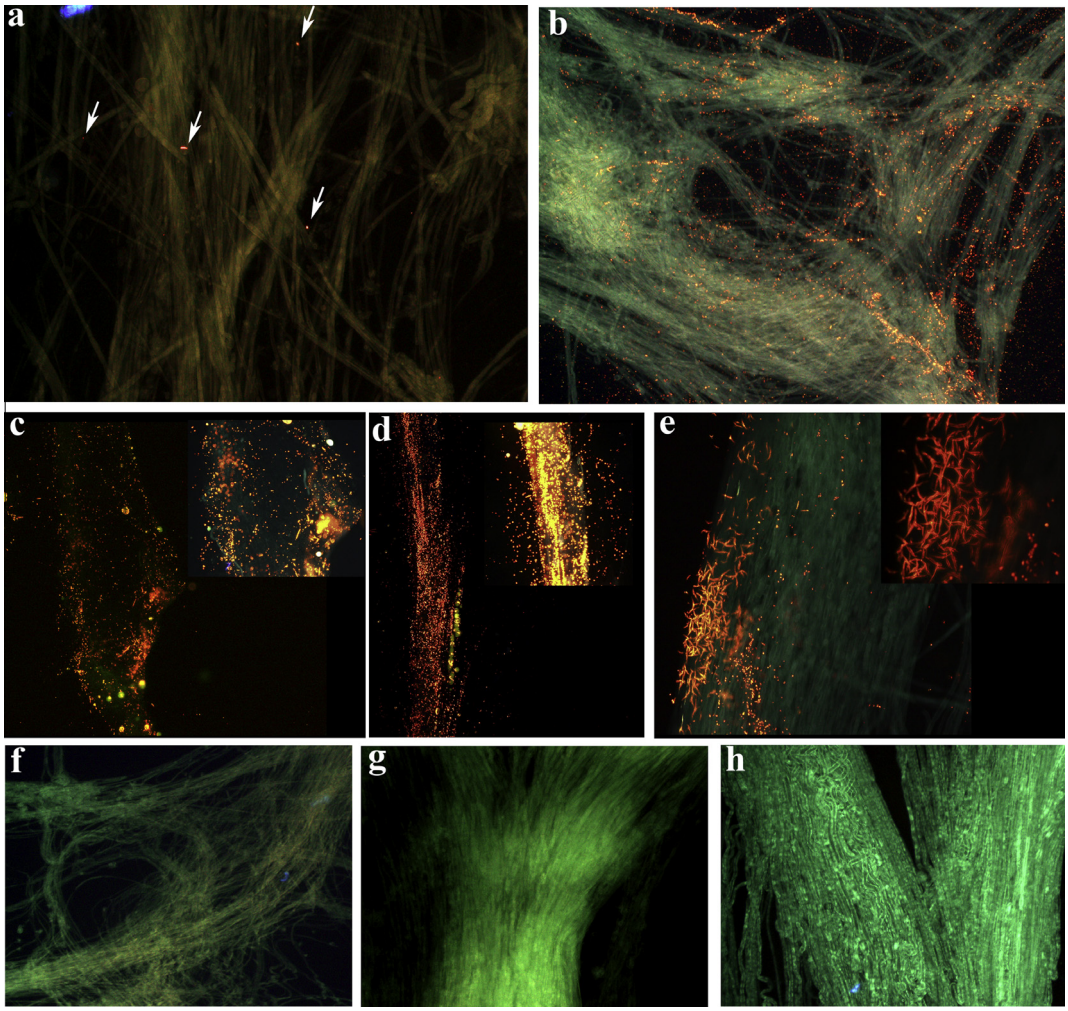

Fig. 9. Histochemical visualization of thrombin activity following crush injury. (a) Fluorescence photomicrographs of sciatic nerves of mice 24 h following crush injury and 1 h following incubation with the substrate Boc-Asp(OBzl)-Pro-Arg-4MβNA. The few yellow reaction products that were generated are indicated by arrows (magnification ×40). (b–e) Massive staining was observed 24 h following incubation (magnification: ×40 (b–d), ×100 (e)). Higher power photomicrographs of pictures c–e are present in the upper right corner of each picture (magnification ×100 (c, d), ×400 (e)). (f and g) Sciatic nerves that underwent crush injury and were incubated in histochemical staining solution containing NAPAP (magnification ×40 (f), ×100 (g)). (h) Uninjured contralateral sciatic nerves that were incubated for 24 h with the substrate Boc-Asp(OBzl)-Pro-Arg-4MβNA (magnification ×100).

cellular level can serve as a strong tool for examining the links between thrombin activity and brain cells. Further experiments using the histochemical method presented here combined with immunohistochemistry techniques are needed to better understand these associations.

In this study we used unfixed cryostat sections for the visualization of thrombin activity in brain slices following tMCAo. We found that in order to retain appropriate levels of thrombin activity in these thin frozen slices, it is required to store the brain in sucrose solution prior to its cutting. This observation is in agreement with relevant literature finding loss of enzyme activity due to freezing, dehydration (Carpenter et al., 1993; Prestrelski et al., 1993; Anchordoquy et al., 2001) and storage at low temperatures for long durations (Paveena et al., 2010, 2011). Sucrose was found to be one of the effective additives for improving the stability of freeze-dried enzymes (Paveena et al., 2010, 2011). In contrast to the brain tissue, the relative rigid structure of the sciatic nerve enables the use of fresh sciatic samples, thus, keeping the initial levels of thrombin activity in the tissue in addition to its original shape.

Chen et al. recently elegantly detected the location of thrombin activity in rat brains following ischemic stroke using a patented cell-penetrating peptide-imaging probe. The probe was infused into the common carotid artery where anterograde flow carries the infused probe into the internal carotid and ultimately to the brain tissue through breakthrough in the BBB (Chen et al., 2012). In contrast to this technique, the histochemical method presented in this study is not dependent on blood flow and reperfusion, thus allowing detection of thrombin activity that is located also in brain tissue supplied by occluded vessels. It is a simple histological method that uses commercially available products and can be performed ex vivo with different tissue types.

In the present study we focused on thrombin due to its highly important role in the nervous system. Thrombin

activity was detected early in experimental autoimmune encephalomyelitis model indicating its potential as a marker for neuroinflammation (Davalos et al., 2014). Furthermore, thrombin activity was significantly elevated in mice brains that underwent minimal traumatic brain injury (mTBI), while injection of PAR1 antagonist completely blocked the amnestic effects of mTBI (Itzekson et al., 2014). Thrombin message and protein were highly expressed in microvessels that were isolated from Alzheimer's disease patient brains but were not detectable in control vessels (Yin et al., 2010). In a rat glioblastoma model thrombin activity was significantly elevated in the tumor and positively correlated with tumor-induced brain edema (Itsekson-Hayosh et al., 2015). In the peripheral system, low concentrations of thrombin were found to be responsible for regeneration of mouse peripheral nerve after its crushing (Balezina et al., 2005) while high concentrations had deleterious effects (Lee et al., 1998). Moreover, mice lacking the thrombin inhibitor protease nexin-1 showed delayed structural and functional recovery after sciatic nerve crush (Lino et al., 2007).

As a key player in the nervous system, thrombin is an attractive target for drug therapy. Argatroban, a specific thrombin inhibitor, has been shown to reduce cell injury and ischemic lesion size after focal cerebral ischemia (McColl et al., 2004; Chen et al., 2012; Lyden et al., 2014). Moreover, administration of nafamostat mesilate during ischemia and reperfusion in a rat model of MCAo reduced thrombin activity and neurological deficit (Chen et al., 2014). In addition, as a coagulation factor, thrombin is a target for prevention of cardioembolic stroke (Verheugt and Granger, 2015). Taken together, the histochemical method presented in this study can serve as an important tool for studying the role of thrombin in physiological and pathological conditions. Consequently it will be useful in the research and development of thrombin-based therapies.

CONCLUSIONS

In summary, we have developed a novel method for detecting the location of thrombin activity and have tested its applicability in mouse brain following tMCAo and teased fibers from mouse sciatic nerve following crush injury. We found compatibility between the results using this novel method and other methods. This simple, time-efficient and accurate method provides a promising direction for thrombin research of central and peripheral nerve diseases.

AUTHOR CONTRIBUTIONS

Doron Bushi designed the study, performed the experiments (*in vitro*, stroke model), analyzed data and wrote the paper.

Orna Gera designed and preformed all the experiments related to the sciatic model and helped with the paper writing.

Genady Kostenich preformed the spectra measurement of the 4MβNA-NSA complexes and helped with the microscopy facilities.

Efrat Shavit-Stein and Ronen Weiss helped with the prepared sections for staining and with the thrombin activity assay.

Joab Chapman and David Tanne supervised the project and revised the manuscript critically for important intellectual content.

All authors gave their approval to the manuscript.

Acknowledgment—The research was supported by institution funding.

REFERENCES

Anchordoquy TJ, Izutsu KI, Randolph TW, Carpenter JF (2001) Maintenance of quaternary structure in the frozen state stabilizes lactate dehydrogenase during freeze-drying. Arch Biochem Biophys 390:35–41.

Back SA, Gorenstein C (1989) Histochemical visualization of neutral endopeptidase-24.11 (enkephalinase) activity in rat brain: cellular localization and codistribution with enkephalins in the globus pallidus. J Neurosci 9:4439–4455.

Balezina OP, Gerasimenko NY, Dugina TN, Strukova SM (2005) Study of neurotrophic activity of thrombin on the model of regenerating mouse nerve. Bull Exp Biol Med 139:4–6.

Bar-Shavit R, Hruska KA, Kahn AJ, Wilner GD (1986) Hormone-like activity of human thrombin. Ann N Y Acad Sci 485:335–348.

Becker D, Ikenberg B, Schiener S, Maggio N, Vlachos A (2014) NMDA-receptor inhibition restores Protease-Activated Receptor 1 (PAR1) mediated alterations in homeostatic synaptic plasticity of denervated mouse dentate granule cells. Neuropharmacology 86:212–218.

Bushi D, Ben Shimon M, Shavit Stein E, Chapman J, Maggio N, Tanne D (2015) Increased thrombin activity following reperfusion after ischemic stroke alters synaptic transmission in the hippocampus. J Neurochem 135:1140–1148.

Bushi D, Chapman J, Katzav A, Shavit-Stein E, Molshatzki N, Maggio N, Tanne D (2013) Quantitative detection of thrombin activity in an ischemic stroke model. J Mol Neurosci 51:844–850.

Carpenter JF, Prestrelski SJ, Arakawa T (1993) Separation of freezing- and drying-induced denaturation of lyophilized proteins using stress-specific stabilization. I. Enzyme activity and calorimetric studies. Arch Biochem Biophys 303:456–464.

Cataldo AM, Nixon RA (1990) Enzymatically active lysosomal proteases are associated with amyloid deposits in Alzheimer brain. Proc Natl Acad Sci U S A 87:3861–3865.

Chapman J (2013) Coagulation in inflammatory diseases of the central nervous system. Semin Thromb Hemost 39:876–880.

Chen B, Cheng Q, Yang K, Lyden PD (2010) Thrombin mediates severe neurovascular injury during ischemia. Stroke 41:2348–2352.

Chen B, Friedman B, Whitney MA, Winkle JA, Lei IF, Olson ES, Cheng Q, Pereira B, Zhao L, Tsien RY, Lyden PD (2012) Thrombin activity associated with neuronal damage during acute focal ischemia. J Neurosci 32:7622–7631.

Chen T, Wang J, Li C, Zhang W, Zhang L, An L, Pang T, Shi X, Liao H (2014) Nafamostat mesilate attenuates neuronal damage in a rat model of transient focal cerebral ischemia through thrombin inhibition. Sci Rep 4:5531.

Coughlin SR (2000) Thrombin signalling and protease-activated receptors. Nature 407:258–264.

Davalos D, Baeten KM, Whitney MA, Mullins ES, Friedman B, Olson ES, Ryu JK, Smirnoff DS, Petersen MA, Bedard C, Degen JL, Tsien RY, Akassoglou K (2014) Early detection of thrombin activity in neuroinflammatory disease. Ann Neurol 75:303–308.

Dolbeare FA, Smith RE (1977) Flow cytometric measurement of peptidases with use of 5-nitrosalicylaldehyde and 4-methoxy-beta-naphthylamine derivatives. Clin Chem 23:1485–1491.

Friedmann I, Faber-Elman A, Yoles E, Schwartz M (1999) Injury-induced gelatinase and thrombin-like activities in regenerating and nonregenerating nervous systems. FASEB J 13:533–543.

Fukusen N, Aoki Y (1996) Purification and characterization of novel trypsin-like serine proteases from mouse spleen. J Biochem 119:633–638.

Hamill CE, Mannaioni G, Lyuboslavsky P, Sastre AA, Traynelis SF (2009) Protease-activated receptor 1-dependent neuronal damage involves NMDA receptor function. Exp Neurol 217:136–146.

Itsekson-Hayosh Z, Shavit-Stein E, Last D, Goez D, Daniels D, Bushi D, Gera O, Zibly Z, Mardor Y, Chapman J, Harnof S (2015) Thrombin activity and thrombin receptor in rat glioblastoma model: possible markers and targets for intervention? J Mol Neurosci 56:644–651.

Itzekson Z, Maggio N, Milman A, Shavit E, Pick CG, Chapman J (2014) Reversal of trauma-induced amnesia in mice by a thrombin receptor antagonist. J Mol Neurosci 53:87–95.

Junge CE, Sugawara T, Mannaioni G, Alagarsamy S, Conn PJ, Brat DJ, Chan PH, Traynelis SF (2003) The contribution of protease-activated receptor 1 to neuronal damage caused by transient focal cerebral ischemia. Proc Natl Acad Sci U S A 100:13019–13024.

Kameda K, Kikkawa Y, Hirano M, Matsuo S, Sasaki T, Hirano K (2012) Combined argatroban and anti-oxidative agents prevents increased vascular contractility to thrombin and other ligands after subarachnoid haemorrhage. Br J Pharmacol 165:106–119.

Kamiya T, Kobayashi Y, Kanaoka K, Nakashima T, Kato Y, Mizuno A, Sakai H (1998) Fluorescence microscopic demonstration of cathepsin K activity as the major lysosomal cysteine proteinase in osteoclasts. J Biochem 123:752–759.

Kawabata A, Kuroda R (2000) Protease-activated receptor (PAR), a novel family of G protein-coupled seven trans-membrane domain receptors: activation mechanisms and physiological roles. Jpn J Pharmacol 82:171–174.

Kawabata S, Miura T, Morita T, Kato H, Fujikawa K, Iwanaga S, Takada K, Kimura T, Sakakibara S (1988) Highly sensitive peptide-4-methylcoumaryl-7-amide substrates for blood-clotting proteases and trypsin. Eur J Biochem 172:17–25.

Lee P, Spector JG, Derby A, Roufa DG (1998) Effects of thrombin and protease nexin-1 on peripheral nerve regeneration. Ann Otol Rhinol Laryngol 107:61–69.

Lino MM, Atanasoski S, Kvajo M, Fayard B, Moreno E, Brenner HR, Suter U, Monard D (2007) Mice lacking protease nexin-1 show delayed structural and functional recovery after sciatic nerve crush. J Neurosci 27:3677–3685.

Lyden P, Pereira B, Chen B, Zhao L, Lamb J, Lei IF, Rajput P (2014) Direct thrombin inhibitor argatroban reduces stroke damage in 2 different models. Stroke 45:896–899.

Maggio N, Cavaliere C, Papa M, Blatt I, Chapman J, Segal M (2013a) Thrombin regulation of synaptic transmission: implications for seizure onset. Neurobiol Dis 50:171–178.

Maggio N, Itsekson Z, Dominissini D, Blatt I, Amariglio N, Rechavi G, Tanne D, Chapman J (2013b) Thrombin regulation of synaptic plasticity: Implications for physiology and pathology. Exp Neurol 247:595–604.

Maggio N, Shavit E, Chapman J, Segal M (2008) Thrombin induces long-term potentiation of reactivity to afferent stimulation and facilitates epileptic seizures in rat hippocampal slices: toward understanding the functional consequences of cerebrovascular insults. J Neurosci 28:732–736.

McColl BW, Carswell HV, McCulloch J, Horsburgh K (2004) Extension of cerebral hypoperfusion and ischaemic pathology beyond MCA territory after intraluminal filament occlusion in C57Bl/6J mice. Brain Res 997:15–23.

Noorbakhsh F, Vergnolle N, Hollenberg MD, Power C (2003) Proteinase-activated receptors in the nervous system. Nat Rev Neurosci 4:981–990.

Paveena S, Kiyoshi K, Naoko HS, Manabu W, Toru S (2011) Stabilizing effects of sucrose–polymer formulations on the activities of freeze-dried enzyme mixtures of alkaline phosphatase, nucleoside phosphorylase and xanthine oxidase. Food Chem 125:1188–1193.

Paveena S, Kiyoshi K, Naoko HS, Manabu W, Toru S (2010) Improvement in the remaining activity of freeze-dried xanthine oxidase with the addition of a disaccharide-polymer mixture. Food Chem 119:209–213.

Prabhakaran S, Ruff I, Bernstein RA (2015) Acute stroke intervention: a systematic review. JAMA 313:1451–1462.

Prestrelski SJ, Arakawa T, Carpenter JF (1993) Separation of freezing- and drying-induced denaturation of lyophilized proteins using stress-specific stabilization. II. Structural studies using infrared spectroscopy. Arch Biochem Biophys 303:465–473.

Rami BK (2012) Direct thrombin inhibitors' potential efficacy in Alzheimer's disease. Am J Alzheimers Dis Other Demen 27:564–567.

Rudolphus A, Stolk J, van Twisk C, van Noorden CJ, Dijkman JH, Kramps JA (1992) Detection of extracellular neutrophil elastase in hamster lungs after intratracheal instillation of E. coli lipopolysaccharide using a fluorogenic, elastase-specific, synthetic substrate. Am J Pathol 141:153–160.

Shavit E, Beilin O, Korczyn AD, Sylantiev C, Aronovich R, Drory VE, Gurwitz D, Horresh I, Bar-Shavit R, Peles E, Chapman J (2008) Thrombin receptor PAR-1 on myelin at the node of Ranvier: a new anatomy and physiology of conduction block. Brain 131:1113–1122.

Smirnova IV, Ma JY, Citron BA, Ratzlaff KT, Gregory EJ, Akaaboune M, Festoff BW (1996) Neural thrombin and protease nexin I kinetics after murine peripheral nerve injury. J Neurochem 67:2188–2199.

Smith RE (1983) Contributions of histochemistry to the development of the proteolytic enzyme detection system in diagnostic medicine. J Histochem Cytochem 31:199–209.

Stein ES, Itsekson-Hayosh Z, Aronovich A, Reisner Y, Bushi D, Pick CG, Tanne D, Chapman J, Vlachos A, Maggio N (2015) Thrombin induces ischemic LTP (iLTP): implications for synaptic plasticity in the acute phase of ischemic stroke. Sci Rep 5:7912.

Sturzebecher J, Walsmann P, Voigt B, Wagner G (1984) Inhibition of bovine and human thrombins by derivatives of benzamidine. Thromb Res 36:457–465.

Suo Z, Citron BA, Festoff BW (2004) Thrombin: a potential proinflammatory mediator in neurotrauma and neurodegenerative disorders. Curr Drug Targets Inflamm Allergy 3:105–114.

Thevenet J, Angelillo-Scherrer A, Price M, Hirt L (2009) Coagulation factor Xa activates thrombin in ischemic neural tissue. J Neurochem 111:828–836.

Verheugt FW, Granger CB (2015) Oral anticoagulants for stroke prevention in atrial fibrillation: current status, special situations, and unmet needs. Lancet 386:303–310.

Xi G, Reiser G, Keep RF (2003) The role of thrombin and thrombin receptors in ischemic, hemorrhagic and traumatic brain injury: deleterious or protective? J Neurochem 84:3–9.

Xue M, Del Bigio MR (2001) Acute tissue damage after injections of thrombin and plasmin into rat striatum. Stroke 32:2164–2169.

Yin X, Wright J, Wall T, Grammas P (2010) Brain endothelial cells synthesize neurotoxic thrombin in Alzheimer's disease. Am J Pathol 176:1600–1606.

(Accepted 29 January 2016)
(Available online xxxx)